The Acquisition Method of Symmetry Chirp Signal Used in LEO Satellite Internet of Things

Yubi Qian, Lu Ma, and Xuwen Liang

***Abstract*— Chirp signal has been used in some fields, like radar and sonar. In recent years, the symmetry chirp signal (SCS) is a kind of revised Long Range (LoRa) chirp signal and proposed to be used in low-earth-orbit (LEO) satellite Internet of Things (IoT) for low-data-rate transmission. However, in terms of the complexity and performance, the traditional acquisition methods to capture SCS (time delay and frequency offset acquisition) will have some limitations in LEO satellite IoT. Thus, this letter presents a new acquisition method to balance the complexity and performance for SCS.**

***Index Terms*— Symmetry chirp signal, LEO satellite IoT, acquisition.**

I. Introduction

CHIRP Spread Spectrum (CSS) modulation has been used commercially in recent years, like IEEE 802.15.4a [1] and LoRa (Long Range) [2]. LoRa modulation (as a kind of CSS) using LoRa chirp signal has been used in terrestrial Internet of Things (IoT) and Symmetry Chirp Signal (SCS) [3] is proposed for Low-Earth-Orbit (LEO) satellite IoT [4] [5]. In LEO satellite communication channel, Doppler Frequency Shift (DFS) (several KHz to tens of KHz) and transmission delay are much bigger than those of terrestrial communication, which will increase the complexity of communication system with the existence of Time Delay (TD) and large DFS [6].

There are two proposed acquisition methods, Fast Acquisition Approach (FAA) [7] and Extended Matched Filter Method (EMFM) [8] for the chirp signal. Both of them can decrease the complexity (power consumption) instead of searching in the limited bandwidth at each time point like the acquisition methods for Direct Sequence Spread Spectrum (DSSS) signal [9] [10]. In this letter, we prefer to study EMFM, because EMFM collects more energy of the useful signal instead of discarding part of that.

Due to importing more noise, EMFM can rough estimate TD and DFS. Hence, accurate acquisition should be necessary for higher acquisition performance. For accurate acquisition of SCS, directly searching DFS in the limited bandwidth called the Direct Searching Method (DSM) is a easy way to implement and Fast Fourier Transform (FFT) method [11] which is used in PN Code for the acquisition is also available. Coarse acquisition for SCS is significant, because it can save more energy for IoT transmitters and receivers. Moreover, due to the traits of SCS, it is easier to realize coarse acquisition. In brief, coarse acquisition with accurate acquisition can realize the tradeoff between performance and power consumption.

Following this Introduction, we are on the analyses of traits of LEO satellite coverage model and SCS comparing with DSSS signal in Section II. Although EMFM is feasible, we want to import less noise and a modified EMFM (mEMFM) is proposed in Section III. mEMFM is considered as the coarse acquisition which is to find the position (TD acquisition) of useful signal, and it combines with FFT to realize TD and DFS acquisition in Section IV. Lastly the conclusion of the whole letter is given in Section V.

Manuscript received April 10, 2019; revised May 28, 2019; accepted June 27, 2019. Date of publication July 2, 2019; date of current version September 10, 2019. The associate editor coordinating the review of this letter and approving it for publication was T. De Cola. *(Corresponding author: Yubi Qian.)*

Y. Qian is with the Shanghai Institute of Microsystem and Information Technology, Chinese Academy of Sciences, Shanghai 200050, China, also with the Shanghai Engineering Center for Microsatellites, Chinese Academy of Sciences, Shanghai 201210, China, and also with the University of Chinese Academy of Sciences, Beijing 100049, China (e-mail: yubiqian@foxmail.com).

L. Ma is with Shanghai SpaceOK Aerospace Technology Co., Ltd., Shanghai 201802, China (e-mail: e_wqs@hotmail.com).

X. Liang is with the Shanghai Engineering Center for Microsatellites, Chinese Academy of Sciences, Shanghai 201210, China (e-mail: 18217631362@163.com).

Digital Object Identifier 10.1109/LCOMM.2019.2926262

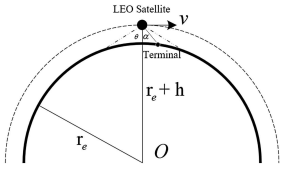

Fig. 1. LEO satellite coverage model.

II. Analyses

A. LEO Satellite Coverage Model

LEO satellite coverage model is shown in Fig.1. Suppose that the satellite orbit is circular, the orbital height is $h(500km$ to $2000km)$, the radius of the earth is r_e, the satellite antenna angle is $\pm\theta$, the geocenter-satellite-terminal angle is α and the speed of the LEO satellite is v, then we can get,

$$v = \sqrt{\frac{\mu}{r_e + h}} \tag{1}$$

where $\mu = 3.986005 \times 10^{14} m^3/s^2$ (gravitational constant of the earth).

$$f_d = \frac{v f_c}{c} sin(\alpha) \tag{2}$$

where $c(= 3 \times 10^8\ m/s)$ is the speed of light, and f_c denotes the carrier frequency.

We define $\eta = |f_d^{max}|/R_s$ (f_d^{max} denotes the maximum DFS and R_s is the symbol rate) and give an example of LEO satellite coverage in TABLE I. From the example, η increases with the increase of carrier frequency and decreases with the increase of the orbital height and Rs.

B. Traits of Symmetry Chirp Signal

The frequency of Traditional Chirp Signal (TCS) shown in [7] [8] varies from f_{min} to f_{max} (up-chirp signal) or from

TABLE I

$h = 800km, r_e = 6400km, \theta = \pi/3, R_s \in \{100bps, 500bps, 1kbps\}$

f_c	$\eta(100bps)$	$\eta(500bps)$	$\eta(1kbps)$
$200MHz$	43	8.6	4.3
$1GHz$	215	43	21.5

f_{max} to f_{min} (down-chirp signal) in one symbol period T_s. For SCS, there are two parts, Positive-Chirp Signal (PCS) and Negative-Chirp Signal (NCS) whose start frequency is the same b_k (Normalized frequency $B_k = G \cdot b_k/B$ where spreading gain is $G = BT_s = 2^{SF}$, SF is spread factor ($SF = 6, 7, 8 \ldots 12$ in LoRa) and $B = f_{max} - f_{min}$ is transmission bandwidth). The chirp rate of TCS is $\mu_{TCS} = \pm\frac{B}{T_s}$, and that of SCS includes $\mu_{PCS} = \frac{2B}{T_s}$ and $\mu_{NCS} = -\frac{2B}{T_s}$.

We refer Ambiguity Function (AF) which denotes the correlation of two kinds of signal in time and frequency domain,

$$AF_{k_1,k_2}(\tau, f_d) = \int_{+\infty}^{+\infty} s_{k_1}(t) s_{k_2}^*(t-\tau) e^{-j2\pi f_d t} dt \quad (3)$$

where τ is TD, f_d is DFS and $s_k(t)$ is k-th kind of signal with the symbol period $T_s(= 1/R_s)$.

- When $s_k(t)$ is DSSS signal, then we can get its maximum auto-correlation at $\tau = 0$,

$$|AF_k^{DSSS}(0, f_d)| = |\frac{sin(\pi f_d T_s)}{\pi f_d T_s}| \quad (4)$$

  The first zero is at $f_d = \pm\frac{1}{T_s} = \pm R_s$.
- When $s_k(t)$ is the TCS, then we can get its maximum auto-correlation at $\tau^* = f_d/\mu_{TCS}$,

$$|AF_k^{TCS}(\tau^*, f_d)| = 1 - |\frac{f_d}{B}| \quad (5)$$

  Though there exists DFS, the maximum auto-correlation of TCS is greater as G increases.
- When $s_k(t)$ is a kind of SCS, then we can get its maximum auto-correlation at $\tau_1^* = f_d/\mu_{PCS}$ and $\tau_2^* = f_d/\mu_{NCS}$,

$$\begin{cases} |AF_k^{SCS}(\tau_1^* \ or \ \tau_2^*, f_d)| \approx \frac{1}{2} - 2|\frac{f_d}{B}|, & B_k \neq 0 \\ |AF_k^{SCS}(\tau_1^* \ or \ \tau_2^*, f_d)| \approx \frac{1}{2} - |\frac{f_d}{B}|, & B_k = 0 \end{cases} \quad (6)$$

  where "$\approx$" means approximate equality and some integral intervals are ignored according to $SectionII$ in [3].

Comparing (4), (5) and (6), we find that the anti-frequency-shift capability of TCS is the best and it is impossible to find the big auto-correlation only by changing TD for DSSS signal. From another perspective, we can make f_d/B to be arbitrarily small by increasing B, i.e. the acquisition of SCS is easier to implement comparing with DSSS signal. Although the maximum auto-correlation of SCS is smaller than that of TCS, we can get the estimated DFS as $f_d^* = (\tau_1^* - \tau_2^*)B/T_s$. These results are fundamental theories to implement TD and DFS acquisition for SCS in next sections.

C. Acquisition

The basic principle of acquisition is to obtain the energy of useful signal $s(t)$ with the period of T_s in time domain and frequency domain by the filter $h(t)$ with the period of T_h.

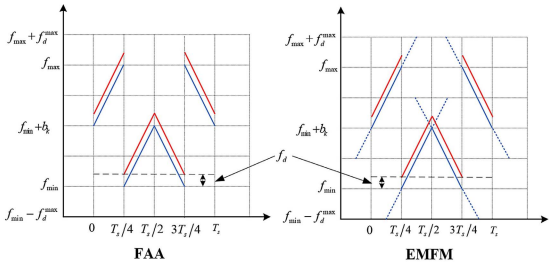

Fig. 2. Frequency-time diagram of FAA filters and extended matched filters, $B_k = G/2$.

In order to simplify the expression, we take the inner product instead of the convolution.

$$\begin{cases} r(t) = s(t)e^{j2\pi f_d t} + n(t) \\ d(\tau) = \int_0^{+\infty} r(t)h^*(t-\tau)dt \end{cases} \quad (7)$$

where $r(t)$ is the received signal and $n(t)$ is Additive Gaussian White Noise (AWGN) with power spectral density $N_0/2$.

Then, when $\tau = 0$, $h(t)$ matches $s(t)e^{j2\pi f_d t}$,

$$d(0) = \sqrt{p_s p_h} T_P + n'(\tau) \quad (8)$$

where p_s and p_h are the power of $s(t)$ and $h(t)$ respectively, T_P is the integral interval of $d(\tau)$ at peak value and $n'(\tau)$ can still be regarded as AWGN with the variance of σ^2.

$$\sigma^2 = \frac{N_0}{2}\int_0^{+\infty} h^2(t)dt = \frac{N_0 p_h T_h}{2} \quad (9)$$

Therefore, $d(0)$ obeys the Gaussian distribution,

$$d(0) \sim N(\sqrt{p_s p_h} T_P, \frac{N_0 p_h T_h}{2}) \quad (10)$$

When a threshold $\lambda_{th} \in (0, 1)$ is given, the missing probability (the probability of missing to detect the useful signal) can be expressed in (11),

$$P_m = p(d(0) < \lambda_{th}\sqrt{p_s p_h} T_P) = Q((1-\lambda_{th})\sqrt{\frac{2p_s T_P^2}{N_0 T_h}}) \quad (11)$$

where $Q(x) = \int_x^{+\infty} e^{-t^2/2}/\sqrt{2\pi}dt$

Especially for accurate acquisition, when $p_s = p_h = \sqrt{E_s/T_s}$ and $T_h = T_s$, $d(0) \sim N(E_s, N_0 E_s/2)$ and $P_m = Q((1-\lambda_{th})\sqrt{2E_s/N_0})$.

III. Coarse Acquisition

A. Fast Acquisition Approach

From the Fig.2, we give the frequency-time diagram of the FAA and EMFM filters where red line denotes the received SCS and blue line is local filter signal. $h_{FAA}(t)$ can be expressed in (12), when $B_k = G/2$,

$$\begin{cases} h_1(t) = s_k(t), & 0 \le t < T_s/4 \\ h_2(t) = s_k(t), & T_s/4 \le t < T_s/2 \\ h_3(t) = s_k(t), & T_s/2 \le t < 3T_s/4 \\ h_4(t) = s_k(t), & 3T_s/4 \le t < T_s \end{cases} \quad (12)$$

The maximum auto-correlation of PCS (AF_p) is at τ_p,

$$\tau_p = arg\max_{\tau}(|\int_0^{T_s/4}(\cdot)_1 dt| + |\int_{T_s/4}^{T_s/2}(\cdot)_2 dt|) \quad (13)$$

The maximum auto-correlation of NCS (AF_p) is at τ_n,

$$\tau_n = arg\max_{\tau}(|\int_{T_s/2}^{3T_s/4}(\cdot)_3 dt| + |\int_{3T_s/4}^{T_s}(\cdot)_4 dt|) \quad (14)$$

where $(\cdot)_m = r(t)h_m^*(t-\tau)$.

Therefore, the estimation of DFS is f_d^*,

$$f_d^* = (\tau_n - \tau_p)B/T_s \quad (15)$$

From (7), (10), (11), (13) and (14), the maximum auto-correlation with FAA obeys the distribution in (16),

$$AF_{FAA} = AF_p + AF_n \sim N((1-2\frac{|f_d|}{B})E_s, \frac{N_0E_s}{2}) \quad (16)$$

Its missing probability is expressed in (17),

$$P_m^{FAA} = Q((1-\lambda_{th})(1-2|f_d|/B)\sqrt{2E_s/N_0}) \quad (17)$$

B. Extended Matched Filter Method

From the Fig.2, we give the frequency-time diagram of the EMFM filter. EMFM extends the bandwidth of matched filter signal to capture the TD and DFS of received signal. In this way, the energies of useful signal, in-band noise and extended-band noise are obtained at the same time. The expansion factor is $\beta = |f_d^{max}|/B = \eta/G$ ($\beta \le 1/2$ in this letter) and the expansion time is $T_E = \beta \cdot T_s/2$.

According to the proposed EMFM, $h_{EMFM}(t)$ of EMFM can be expressed in (18), when $B_k = G/2$,

$$\begin{cases} h_1(t) = \sqrt{p}F^+(b_k - f_d^{max}), & -T_E \le t < T_s/4+T_E \\ h_2(t) = \sqrt{p}F^+(-f_d^{max}), & T_s/4-T_E \le t < T_s/2+T_E \\ h_3(t) = \sqrt{p}F^-(b_k + f_d^{max}), & T_s/2-T_E \le t < 3T_s/4+T_E \\ h_4(t) = \sqrt{p}F^-(B + f_d^{max}), & 3T_s/4-T_E \le t < T_s+T_E \end{cases} \quad (18)$$

where p denotes the power of SCS, $p = E_s/T_s$ and E_s is the energy of one symbol,

$$F^+(f) = e^{j2\pi(\frac{B}{T_s}t^2+f_{min}+f)}, \quad F^-(f) = e^{j2\pi(-\frac{B}{T_s}t^2+f_{min}+f)}$$

Similar with FAA, the results are shown in (19) with (10), (11), (13), (14), (15) and (18).

$$\begin{cases} f_d^* = (\tau_n - \tau_p)B/T_s \\ AF_{EMFM} \sim N(E_s, (1+4\beta)N_0E_s/2) \\ P_m^{EMFM} = Q((1-\lambda_{th})\sqrt{2E_s/(1+4\beta)N_0}) \end{cases} \quad (19)$$

The acquisition simulations of FAA and EMFM are shown in Fig.3 by MATLAB. In the simulations, $f_d \sim U(-|f_d^{max}|, |f_d^{max}|)$. From the simulations, we find that EMFM is better than FAA. Especially when f_d is larger, FAA will lose more energy of useful signal and the acquisition performance of FAA is wrose than that of EMFM.

C. Modified Extended Matched Filter Method

The whole EMFM process is named as $EMFM$ module which consists of one input (received signal) and four outputs (two kinds of estimated TD and their AFs). In LEO satellite communication channel, DFS is either positive or negative in the limited band for the certain signal, which means that we don't need to extend upper-limit and lower-limit bandwidth at the same time. Hence, we can modify the extended matched filter and call this method as modified EMFM (mEMFM).

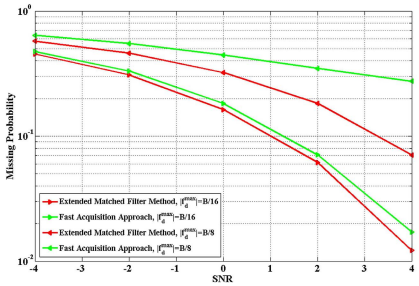

Fig. 3. Performance comparison of FAA and EMFM, $B_k = G/2, SF = 6$ and $\lambda_{th} = 0.8$.

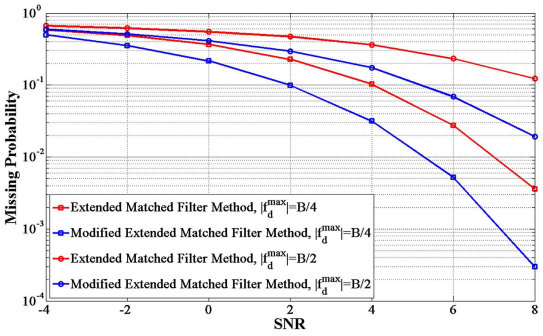

Fig. 4. Missing probability of acquisition with EMFM and mEMFM for $SF = 6$, $B_k = G/2$ and $\lambda_{th} = 0.8$.

$mEMFM-1$ module uses the modified extended matched filter for the positive DFS only with upper-limit extended bandwidth,

$$\begin{cases} h_1(t) = \sqrt{p}F^+(b_k), & 0 \le t < T_s/4+T_E \\ h_2(t) = \sqrt{p}F^+(0), & T_s/4 \le t < T_s/2+T_E \\ h_3(t) = \sqrt{p}F^-(b_k + f_d^{max}), & T_s/2 \le t < 3T_s/4+T_E \\ h_4(t) = \sqrt{p}F^-(B + f_d^{max}), & 3T_s/4 \le t < T_s+T_E \end{cases} \quad (20)$$

$mEMFM-2$ module uses the modified extended matched filter for the negative DFS only with lower-limit extended bandwidth,

$$\begin{cases} h_1(t) = \sqrt{p}F^+(b_k - f_d^{max}), & -T_E \le t < T_s/4 \\ h_2(t) = \sqrt{p}F^+(-f_d^{max}), & T_s/4-T_E \le t < T_s/2 \\ h_3(t) = \sqrt{p}F^-(b_k), & T_s/2-T_E \le t < 3T_s/4 \\ h_4(t) = \sqrt{p}F^-(B), & 3T_s/4-T_E \le t < T_s \end{cases} \quad (21)$$

Similar with (19), the results are shown in (22) with (10), (11), (13), (14), (15), (20) and (21), when $B_k = G/2$,

$$\begin{cases} f_d^* = (\tau_n - \tau_p)B/T_s \\ AF_{mEMFM} \sim N(E_s, (1+2\beta)N_0E_s/2) \\ P_m^{mEMFM} = Q((1-\lambda_{th})\sqrt{2E_s/(1+2\beta)N_0}) \end{cases} \quad (22)$$

With the Monte-Carlo methods for the simulations of acquisition performance, we compare EMFM and mEMFM in terms of the missing probability shown in Fig.4. From the figure, we find that the smaller β is, the smaller the missing probability is for both of them. Due to bringing in less noise

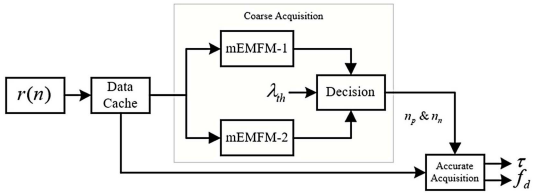

Fig. 5. The whole process of acquisition for SCS.

expressed in (19) and (22), the performance of mEMFM is better than that of EMFM illustrated in Fig.4.

Besides, when $B_k = 0$, $2|fd|$ in (17), 4β in (19) and 2β in (22) change to $|fd|$, 2β, β respectively. In other word, SCS with $B_k = 0$ inherently has better acquisition performance.

IV. The Whole Acquisition Process

For LEO satellite IoT terminals, their daily communication duty cycles are very low and they can't always be in the state of accurate acquisition, which will cause much power consumption. mEMFM is a better method for coarse acquisition before accurate acquisition in order to realize power save.

The whole process of acquisition for SCS is shown in Fig.5 with discrete sequences. In the figure, $r(n)$ is the received sequence, and $n_p\&n_n$ are the TD estimation for PCS and NCS.

The methods of accurate acquisition include DSM and FFT method and the FFT method is applied in this letter. We let $N_E = T_E/T_{sam}$ and $N = T_s/T_{sam}$ where T_{sam} is the sampling period. After obtaining n_p and n_n, accurate acquisition starts to work at $n_0 \in [\frac{n_p+n_n}{2}, \frac{n_p+n_n}{2} + N_E]$ when $n_p \geq n_n$ and at $n_0 \in [\frac{n_p+n_n}{2} - N_E, \frac{n_p+n_n}{2}]$ when $n_p < n_n$. Actually, Accurate acquisition between $[\frac{n_p+n_n}{2} - N_E, \frac{n_p+n_n}{2} + N_E]$ could be better, because we don't need to take the false probability of the estimation with $n2_p\&n2_n$ $(n1_p\&n1_n)$ into account when $AF1_p + AF1_n > (<) AF2_p + AF2_n$, which improves the probability of finding the correct position of useful signal.

According to (7), we get the sequence c_{n_0} after correlation, $FFT_{n_o}(\Omega)$ after FFT and estimations of TD and DFS,

$$\begin{cases} c_{n_0}(n) = r(n-n_0)s_k^*(n), & 0 \leq n < N-1 \\ F_{n_o}(\Omega) = FFT(c_{n_0}) \\ n_0^* = arg\max\limits_{n_o} max(F_{n_o}(\Omega)), & \Omega^* = arg\max\limits_{\Omega} F_{n_0^*}(\Omega) \end{cases} \tag{23}$$

The performance simulations of mEMFM, mEMFM with FFT and pure FFT method are shown in Fig.6. From the figure, the performance of mEMFM with FFT is much better than that of mEMFM and not better than that of pure FFT method. Since $p(y) = p(x)p(y|x)+p(\overline{x})p(y|\overline{x})$ where x means correct TD synchronization and x denotes correct TD&DFS synchronization, $p(y)$ can be expressed the correct probability of pure FFT method while $p(x)p(y|x)$ is that of mEMFM with FFT. Therefore, the performance of pure FFT method is better than that of mEMFM with FFT for $p(y) > p(x)p(y|x)$.

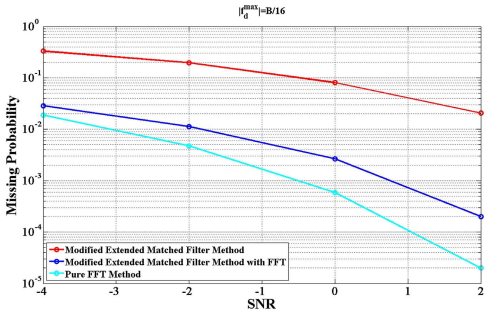

Fig. 6. The performance of coarse acquisition, coarse acquisition with FFT and pure FFT method for $SF = 6$, $B_k = G/2$ and $\lambda_{th} = 0.8$.

Hence, the proposed method (mEMFM with FFT) can balance the power consumption and acquisition performance.

V. Conclusion

This letter is on the research of the acquisition method for SCS in LEO satellite IoT. We compare SCS with DSSS signal and find that SCS has better anti-frequency-shift capacity, which facilitates to realize acquisition with a low-power method. Then, we modify the EMFM as mEMFM and combine that with accurate acquisition to propose a complete acquisition method for SCS in LEO satellite IoT. In further research, we will keep on the research of acquisition technology in multiple access channel [12] for LEO satellite IoT communications.

References

[1] *IEEE Standard for Information Technology—Local and Metropolitan Area Networks—Specific Requirements– Part 15.4: Wireless Medium Access Control (MAC) and Physical Layer (PHY) Specifications for Low-Rate Wireless Personal Area Networks (WPANs): Amendment 1: Add Alternate PHYs*, IEEE Standard 802.15.4a-2007, 2007.

[2] *LoRaWan*. Accessed: Jan. 1, 2019. [Online]. Available: https://lora-alliance.org/sites/default/files/2018-04/lorawantm specification-v1.1.pdf

[3] Y. Qian, L. Ma, and X. Liang. "Symmetry chirp spread spectrum modulation used in LEO satellite Internet of Things," *IEEE Commun. Lett.*, vol. 22, no. 11, pp. 2230–2233, Nov. 2018.

[4] Z. Qu, G. Zhang, H. Cao, and J. Xie, "Leo satellite constellation for Internet of Things," *IEEE Access*, vol. 5, pp. 18391–18401, 2017.

[5] D. Hu, L. He, and J. Wu, "A novel forward-link multiplexed scheme in satellite-based Internet of Things," *IEEE Internet Things J.*, vol. 5, no. 2, pp. 1265–1274, Apr. 2018.

[6] Q. Liu, "Frequency synchronization in global satellite communications systems," *IEEE Trans. Commun.*, vol. 51, no. 3, pp. 359–365, Mar. 2003.

[7] T. Wang, H. Huan, C. Feng, and R. Tao, "Chirp noise waveform aided fast acquisition approach for Large Doppler shifted TT&C system," in *Proc. IEEE Global Commun. Conf. (GLOBECOM)*, 2015, pp. 1– 6.

[8] R. Kadlimatti and A. T. Fam, "Doppler detection for linear FM waveform using extended matched filter," in *Proc. IEEE Radar Conf.*, May 2016, pp. 1–5.

[9] S. Ding, Z. Yi, H. Liu, and X. Liang, "An improved code acquisition scheme for band-limited DSSS systems with sampling offset," *IEEE Commun. Lett.*, vol. 16, no. 8, pp. 1169–1172, Aug. 2012.

[10] A. A. D'Amico and M. Morelli, "Frequency estimation and timing acquisition in the uplink of a DS-CDMA system," *IEEE Trans. Commun.*, vol. 52, no. 10, pp. 809–819, Oct. 2004.

[11] P. Huang and B.-F. Zu, "Performance analysis of PN code acquisition using fast Fourier transform," in *Proc. 5th Int. Conf. Wireless Commun., Netw. Mobile Comput.*, Oct. 2009, pp. 1–5.

[12] O. D. R. Herrero and R. De Gaudenzi, "High efficiency satellite multiple access scheme for machine-to-machine communications," *IEEE Trans. Aerosp. Electron. Syst.*, vol. 48, no. 4, pp. 2961–2989, Oct. 2012.